Vamp-7–dependent secretion at the immune synapse regulates antigen extraction and presentation in B-lymphocytes

Dorian Obino[a,†,‡], Jheimmy Diaz[b,†], Juan José Sáez[b], Jorge Ibañez-Vega[b], Pablo J. Sáez[a], Martina Alamo[b], Danielle Lankar[a], and Maria-Isabel Yuseff[b,*]

[a]INSERM, U932 Immunité et Cancer, Institut Curie, PSL Research University, 75005 Paris, France; [b]Department of Cellular and Molecular Biology, Faculty of Sciences, Pontificia Universidad Católica de Chile, Santiago 8331150, Chile

ABSTRACT **Recognition of surface-tethered antigens (Ags) by B-cells leads to the formation of an immune synapse that promotes Ag uptake for presentation onto MHC-II molecules. Extraction of immobilized Ags at the immune synapse of B-cells relies on the local secretion of lysosomes, which are recruited to the Ag contact site by polarization of their microtubule network. Although conserved polarity proteins have been implicated in coordinating cytoskeleton remodeling with lysosome trafficking, the cellular machinery associated with lysosomal vesicles that regulates their docking and secretion at the synaptic interface has not been defined. Here we show that the v-SNARE protein Vamp-7 is associated with Lamp-1$^+$ lysosomal vesicles, which are recruited and docked at the center of the immune synapse of B-cells. A decrease in Vamp-7 expression does not alter lysosome transport to the synaptic interface but impairs their local secretion, a defect that compromises the ability of B-cells to extract, process, and present immobilized Ag. Thus our results reveal that B-cells rely on the SNARE protein Vamp-7 to promote the local exocytosis of lysosomes at the immune synapse, which is required for efficient Ag extraction and presentation.**

Monitoring Editor
Jean E. Gruenberg
University of Geneva

Received: Oct 18, 2016
Revised: Jan 31, 2017
Accepted: Feb 1, 2017

INTRODUCTION

To become fully activated, B-cells must efficiently capture external antigens (Ags) and present them as peptide fragments to primed CD4$^+$ T-cells. This process allows the establishment of T-B cooperation, which generates the secondary stimuli required for B-cells to differentiate into high-affinity antibody-producing plasma cells and develop into memory B-cell populations (Mitchison, 2004). Antigens immobilized on the surface of specialized presenting cells are particularly efficient in triggering B-cell activation in vivo (Carrasco and Batista, 2007; Junt *et al.*, 2007). Their engagement by the B-cell receptor (BCR) leads to the formation of an immune synapse (IS; Batista *et al.*, 2001), where both signaling cascades and Ag extraction are tightly coordinated (Tolar *et al.*, 2008). By exerting a rapid spreading and contraction response (Fleire *et al.*, 2006), B-cells efficiently gather immobilized Ag into BCR microclusters, which subsequently converge into a central cluster by the concerted actions of cortical actin cytoskeleton rearrangements (Westerberg *et al.*, 2001; Arana *et al.*, 2008) and the microtubule motor, dynein (Schnyder *et al.*, 2011; Reversat *et al.*, 2015). BCR-Ag complexes are then internalized into major histocompatibility complex class II (MHC-II)–containing endolysosome compartments, where Ag processing takes place (Lankar *et al.*, 2002).

Although extensive progress has been made in elucidating how signaling and actin remodeling are regulated at the synaptic interface, fewer studies have focused on regulatory aspects of membrane trafficking and its effect on the extraction of Ag at the IS of B-cells. In this perspective, two nonexclusive mechanisms have been proposed. The first one involves myosin IIA–mediated pulling forces that trigger invagination of antigen-containing membranes, which are internalized into clathrin-coated pits

This article was published online ahead of print in MBoC in Press (http://www.molbiolcell.org/cgi/doi/10.1091/mbc.E16-10-0722) on February 8, 2017.

†These authors contributed equally to this work.

‡Present address: Pathogenesis of Vascular Infections Unit, INSERM, Institut Pasteur, 75015 Paris, France.

*Address correspondence to: Maria-Isabel Yuseff (myuseff@bio.puc.cl).

Abbreviations used: Ag, antigen; BCR, B-cell receptor; IS, immune synapse; MHC-II, major histocompatibility complex class II; MTOC, microtubule-organizing center.

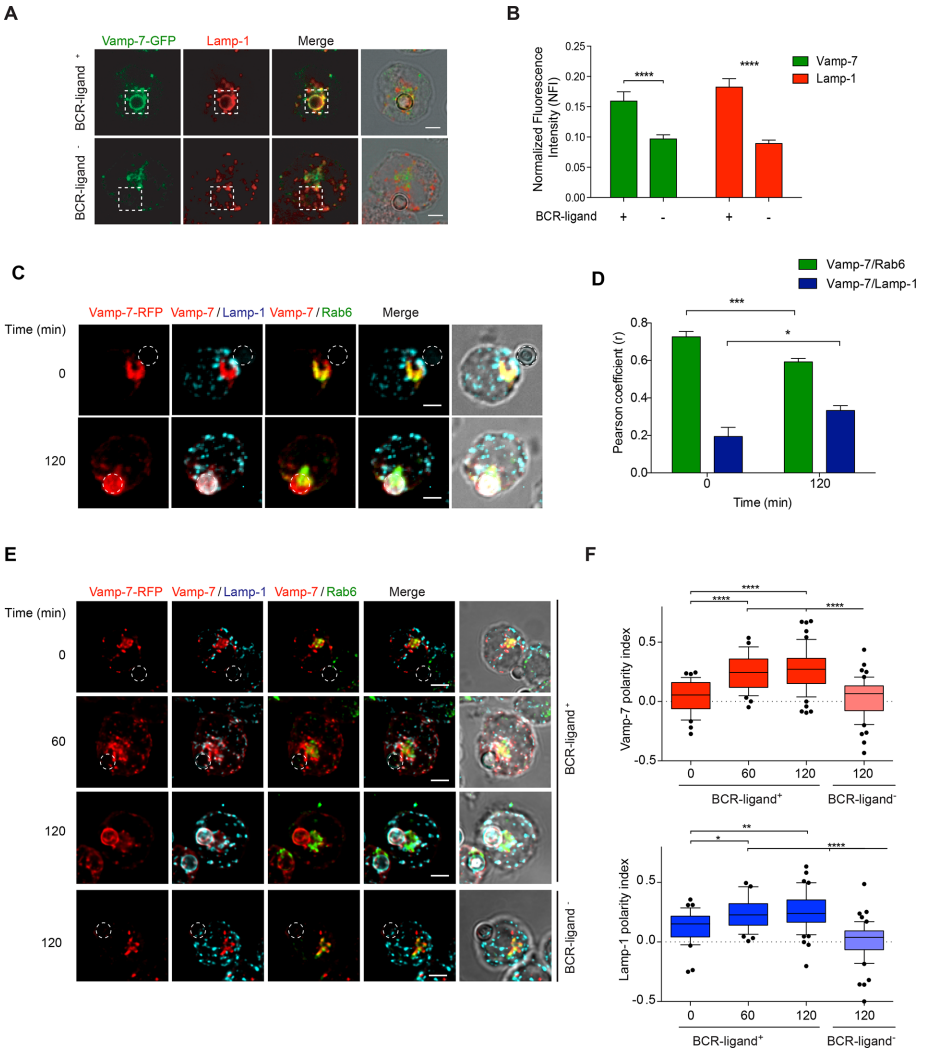

FIGURE 1: Vamp-7$^+$/Lamp-1$^+$ lysosomes are recruited to the IS of B-cells. (A) Immunofluorescence staining of lysosomes (Lamp-1) in B-cells expressing Vamp-7–GFP incubated with BCR-ligand$^+$ or BCR-ligand$^-$ beads for 2 h. Dashed squares indicate the area where Vamp-7-GFP and Lamp-1 signals were measured. (B) Quantification of Lamp-1 and Vamp-7 mean fluorescence intensity recruited to the antigen-contact site, vvv to the total amount of Lamp-1$^+$ lysosomes or Vamp-7$^+$ vesicles, respectively, in the entire cell (NFI). $n \geq 36$; three independent experiments. (C) *Z*-planes of confocal images and (E) fluorescence images of B-cells expressing Vamp-7–RFP activated as described and stained for Lamp-1 and Rab6. Scale bar, 3 μm. (D) Pearson's *r* for Vamp-7/Rab6 or Vamp-7/Lamp-1 in nonactivated and activated cells ($n \geq 14$; two independent experiments). (F) Polarity indexes obtained for Lamp-1$^+$ and Vamp-7$^+$ vesicles using single-cell analysis. $n \geq 36$; three independent experiments. Analysis of variance (ANOVA) followed by Sidak's multiple comparison test, *$p < 0.05$; **$p < 0.01$; ***$p < 0.001$; ****$p < 0.0001$.

In eukaryotes, the fusion of vesicles to target membranes relies on transmembrane proteins containing cytoplasmic soluble *N*-ethylmaleimide–sensitive protein-attachment protein receptor (SNARE) domains (Jahn and Scheller, 2006; Sudhof and Rothman, 2009). SNARE molecules promote docking, priming, and fusion of opposing membranes and are essential throughout the exocytic and endocytic pathways (Novick *et al.*, 2006). Cells of the immune system depend on SNARE proteins to perform effector functions, such as the release of inflammatory molecules, cytokines, degranulation, and local exocytosis of secretory granules (Stow *et al.*, 2006). However, in B-cells, their role has not been addressed. We focused on the vesicle (v)-SNARE protein Vamp-7 (also known as Ti-Vamp), which is involved in the exocytosis of secretory lysosomes in various cell types (Braun *et al.*, 2004; Alberts *et al.*, 2006; Marcet-Palacios *et al.*, 2008), and determined whether it was implicated in lysosome secretion at the IS of B-cells. Our results show that Vamp-7–dependent exocytosis of lysosomes at the IS is critical for B-lymphocytes to acquire their Ag presentation function.

RESULTS AND DISCUSSION

Vamp-7$^+$ lysosomes are recruited to the B-cell immune synapse

We sought to determine the cellular machinery involved in local lysosome secretion at the synaptic membrane of B-cells and focused on the v-SNARE protein Vamp-7. Quantitative PCR and Western blot analysis showed that Vamp-7 was expressed in B-cells (Supplemental Figure S1, A and B). Because no Vamp-7 antibody was available for immunofluorescence analysis, we used previously characterized Vamp-7–green fluorescent protein (GFP)/monomeric red fluorescent protein (mRFP) constructs (Martinez-Arca *et al.*, 2000) to study its localization and dynamics during B-cell activation with immobilized Ag. B-cells expressing Vamp-7–GFP were incubated for 2 h with activating beads containing F(ab')$_2$ anti–immunoglobulin G (IgG), termed BCR-ligand$^+$, or nonactivating beads containing F(ab')$_2$ anti-IgM, termed BCR-ligand$^-$. This system was previously used to mimic the interaction of B-cells with immobilized antigen (Yuseff *et al.*, 2011; Yuseff and Lennon-Dumenil, 2013; Obino *et al.*, 2016) and will be referred to as the IS hereafter. When ectopically expressed in B-cells, Vamp-7–GFP labeled the Lamp-1$^+$ lysosomes that polarized toward the IS (Figure 1A). Quantification of Lamp-1 and Vamp-7 fluorescence signals at the cell–bead interface showed that both markers were enriched at the IS only when stimulated with activating beads (Figure 1B), demonstrating that this process was dependent on BCR engagement. In other cell types, Vamp-7 is found mainly in late endosomes and lysosomes, as well as at the Golgi apparatus, and is involved in both secretory and endocytic pathways (Natkanski *et al.*, 2013). The second one is based on the local secretion of lysosomes that release proteases and acidify the synaptic cleft, allowing antigen extraction (Yuseff *et al.*, 2011, 2013). The latter is supported by results showing that interfering with the recruitment and secretion of MHC-II–containing lysosomes at the IS of B-cells severely impairs the extraction and presentation of immobilized Ag (Yuseff *et al.*, 2011). Polarized lysosome transport is guided by repositioning of the microtubule-organizing center (MTOC) toward the IS, which relies on conserved polarity proteins, such as PAR3/aPKC and Cdc42 (Yuseff *et al.*, 2011; Yuseff and Lennon-Dumenil, 2015; Reversat *et al.*, 2015). However, the molecular basis for the docking and/or secretion of lysosomes at the synaptic membrane has not been defined.

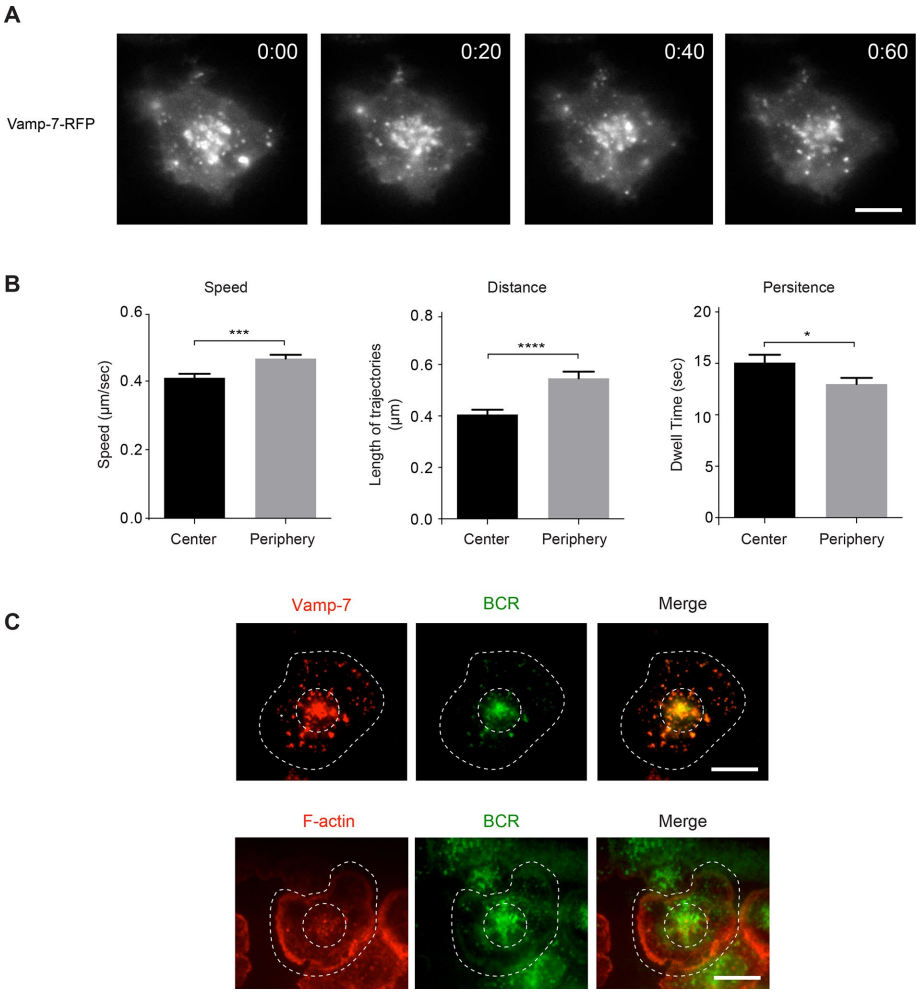

FIGURE 2: Vamp-7$^+$ vesicles accumulate at the center of the synapse formed by B-cells. (A) TIRFM images of Vamp-7-RFP$^+$ vesicles in B-cells plated for 30 min on antigen-coated slides. Scale bar, 5 μm. Time is shown in minutes:seconds. (B) Quantification of dynamic parameters of Vamp-7$^+$ vesicle pools at the central and peripheral regions of the IS. $n = 7$, total >300 trajectories. Unpaired *t* test. Speed $p = 0.0004$, distance $p < 0.0001$, persistence $p = 0.0302$. (C) TIRFM images of B-cells expressing Vamp-7–RFP$^+$ plated onto Ag-coated slides for 1 h. Vamp-7–RFP or F-actin (phalloidin) and BCR. Scale bar, 5 μm.

(Chaineau *et al.*, 2009). To characterize further the subcellular localization of Vamp-7 in B-cells, we performed an immunofluorescence analysis in which Vamp-7-GFP–expressing B-cells were activated for different time points and stained for Rab6 (Golgi apparatus) and Lamp-1 (lysosomes). Imaging analysis showed that in resting conditions, Vamp-7 mainly colocalized with Rab6 and to a lesser extent with Lamp-1$^+$ vesicles (Pearson's $r = 0.73$ and 0.19, respectively). On activation with immobilized Ag, colocalization of Vamp-7 with Rab6 decreased, whereas it increased with Lamp-1$^+$ vesicles (Pearson's $r = 0.59$ and 0.33, respectively; Figure 1, C and D), suggesting that Vamp-7$^+$ vesicles were mobilized from the Golgi apparatus toward the IS, where they coalesced with Lamp-1$^+$ vesicles (Figure 1C). Accordingly, polarity indexes calculated for Vamp-7$^+$ and Lamp-1$^+$ vesicles showed that both pools were concomitantly recruited to the IS upon incubation with BCR-ligand$^+$ beads (Figure 1, E and F) and displayed significant correlation, suggesting that their spatial distributions follow a similar behavior upon BCR activation (Supplemental Figure S1E). Of importance, polarization was not observed in B-cells stimulated with nonactivating beads (Figure 1, E and F).

Lysosome secretion at the B-cell synapse relies on the polarization of the microtubule network, which is promoted by conserved polarity proteins such as Cdc42 and its effector, aPKCζ. Given that Vamp-7$^+$ vesicles at the IS were equally labeled for Lamp-1, we investigated whether their polarization to the IS was also dependent on Cdc42, as observed for Lamp-1$^+$ lysosomes (Yuseff *et al.*, 2011). Accordingly, polarized recruitment of Vamp-7$^+$ vesicles at the cell–bead interface was also compromised in Cdc42-knockdown cells (Supplemental Figure S1F); hence BCR engagement with immobilized antigens triggers the polarized recruitment of both Vamp-7$^+$ and Lamp-1$^+$ vesicles to the IS in a Cdc42-dependent manner.

Vamp-7 regulates the local secretion of lysosomes at the B-cell synapse

We next characterized Vamp-7$^+$ lysosome dynamics at the IS by using total internal reflection fluorescence microscopy (TIRFM). For this, B-cells expressing Vamp-7–RFP were plated onto glass slides coated with specific BCR ligands for various time periods and 1-min movies were acquired. Vamp-7–labeled lysosomes were detected in the evanescent field, where local vesicle clustering was frequently observed at the center of the surface in contact with the immobilized Ag (Figure 2A and Supplemental Movie S1). Quantification of vesicle dynamics revealed that mean velocity levels of Vamp-7$^+$ vesicles at the cell periphery were slightly but significantly higher than with the central pool, which displayed slower movements, as well as higher persistence times and shorter trajectories (Figure 2B), suggesting that they were docked at the plasma membrane within an area that most likely corresponds to the central supramolecular activation complex (cSMAC). Indeed, TIRFM imaging showed that Vamp-7$^+$ vesicles localized closely with gathered BCRs, a marker of the cSMAC, and not with the actin-rich area, localized toward the synapse periphery (Figure 2C). Thus BCR engagement by surface-tethered Ag triggers the stable recruitment of Vamp-7$^+$ vesicles at the center of the IS.

To investigate whether Vamp-7 was involved in the secretion of lysosomes at the IS, we assessed the effects of small interfering RNA (siRNA)–mediated silencing of Vamp-7 expression. Whereas one of the siRNAs did not significantly affect the levels of Vamp-7 transcripts (siVamp-7-A), the second one decreased their levels by ~50% (siVamp-7-B; Supplemental Figure S1, A–D) and was thus used for subsequent functional assays. Vamp-7 silencing had no major effect on MTOC and lysosome polarized transport towards the cell–bead interface (Figure 3, A–C). However, Vamp-7–knockdown cells lacked the typical Lamp-1$^+$ ring that decorated activating beads after prolonged periods of incubation (1–2 h) between cells and beads (Figure 3D), suggesting that Vamp-7 is involved in the docking and/or fusion of lysosomes with the plasma membrane. To explore this hypothesis further, we used TIRFM to monitor cathepsinD-RFP$^+$

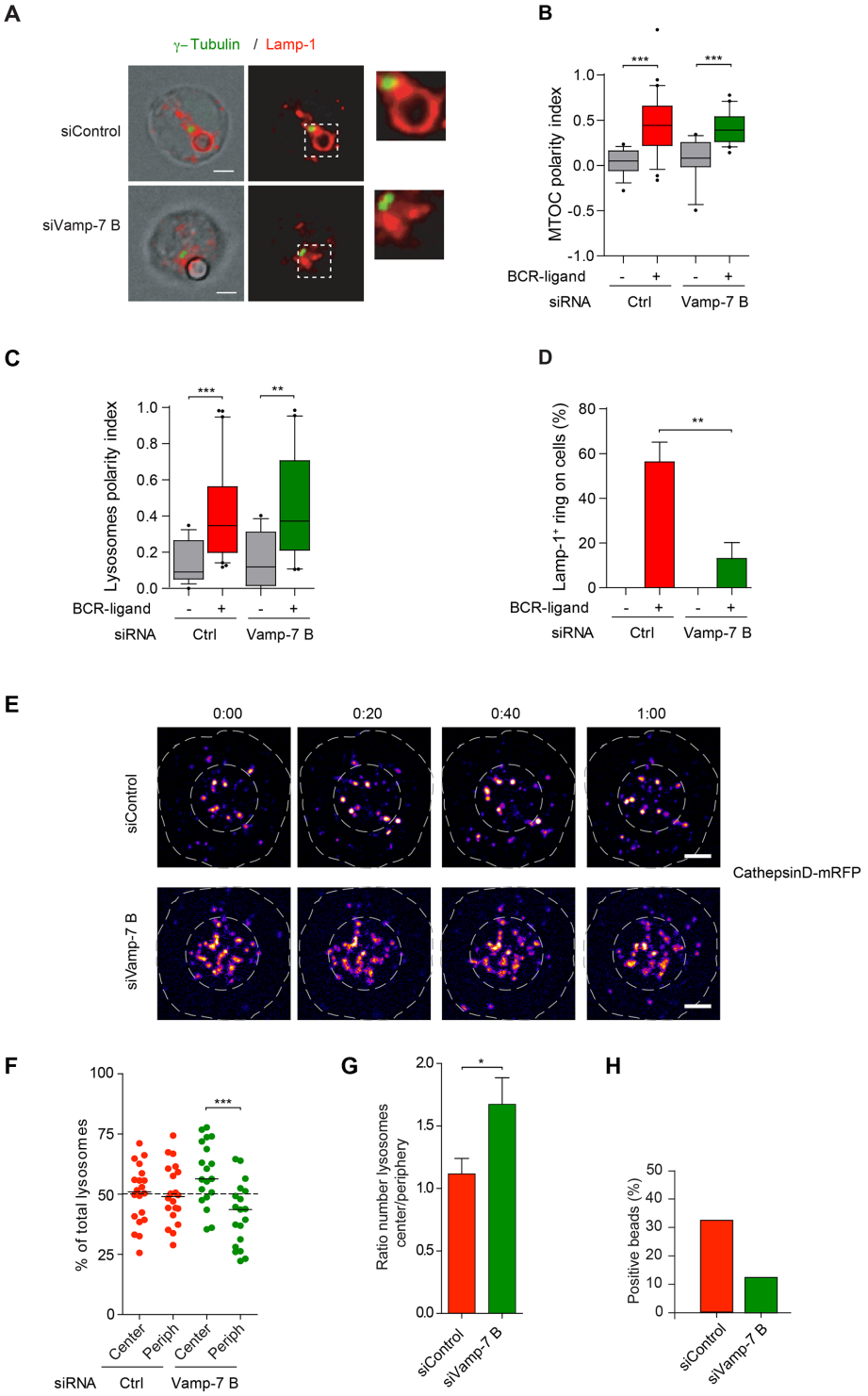

FIGURE 3: Lysosome exocytosis at the IS of B-cells requires Vamp-7. (A) Confocal images of Control and Vamp-7–silenced B-cells incubated with BCR-ligand$^+$ beads for 2 h. Cells were stained against γ-tubulin and Lamp-1. Scale bar, 3 μm. Dashed squares show the area around the Ag-coated bead that was magnified. (B, C) MTOC and lysosome polarity indexes and (D) quantification of Lamp-1$^+$ rings around Ag-coated beads in control and Vamp-7–silenced cells after 2 h of activation; ≥20 cells/condition; two independent experiments. (B) siCtrl $p < 0.0001$; siVamp-7 B $p < 0.0001$. Unpaired *t* test. (C) siCtrl $p = 0.0006$; siVamp-7 B $p = 0.0029$. Unpaired *t* test. (D) $p = 0.0013$. Mann–Whitney test. (E) TIRFM images showing the time-projection of cathepsinD-mRFP$^+$ vesicles in control and Vamp-7–silenced B-cells. Scale bar, 5 μm. (F, G) Quantification of the percentage and the ratio of lysosomes in the central region (Center) vs. the periphery (Periph) of images shown in E. (F) Twenty cells for siControl and 19 cells for siVamp-7; four independent experiments. ***$p < 0.05$, ANOVA followed by a Bonferroni multiple comparison test. (G) *$p = 0.0295$, unpaired *t* test. (H) Quantification of the percentage of control and Vamp-7–silenced B-cells engaged with CypHer5E Ag-coated beads that were positive for CypHer5E fluorescence (mean fluorescence intensity [MFI] of the bead >10% above background levels) after an incubation of 90 min; >180 cells/condition. $p = 6.85 \times 10^{-7}$, Kolmogorov–Smirnov test.

lysosomes at the IS of control and Vamp-7–silenced cells seeded on antigen-coated slides. Unexpectedly, our results revealed that whereas control cells exhibited an equal proportion of lysosomes at the center and periphery of the IS, Vamp-7–knockdown cells presented a significant increase in the proportion of lysosomes located within the center of the IS (Figure 3, E–G, and Supplemental Movies S2 and S3). This observation suggests that in Vamp-7–knockdown cells, lysosomes could be accumulating at the center of the IS as a result of their impaired fusion and secretion with the plasma membrane. To assess directly the effect of Vamp-7 silencing on lysosome secretion at the IS, we coupled BCR ligand to CypHer5E, a dye used to measure local pH acidification at the IS in B-cells, which correlates with exocytosis of lysosomes (Yuseff *et al.*, 2011). We observed that Vamp-7–silenced cells triggered fewer fluorescence signals at the interface between B-cells and CypHer5E-coated activating beads (Figure 3H), suggesting that Vamp-7 regulates the exocytosis of lysosomes at the IS.

Antigen presentation is impaired in Vamp-7–silenced B-lymphocytes

Having shown that lysosome secretion at the B-cell synapse depends on Vamp-7, we next investigated whether this v-SNARE was required for the extraction and presentation of immobilized Ag. First, we evaluated Ag extraction by measuring the fluorescence signal of ovalbumin (OVA) remaining on activating (BCR-ligand$^+$) or nonactivating (BCR-ligand$^-$) beads after their interaction with control or Vamp-7–silenced cells. As expected, higher levels of OVA were detected on beads interacting with Vamp-7–silenced B-cells then in control cells, even after 120 min of incubation (Figure 4, A and B). Of importance, Vamp-7–knockdown cells displayed similar BCR surface levels as control cells (Supplemental Figure S1G), suggesting that defects in Ag extraction did not result from a diminished capacity to interact with Ag. In addition, we did not observe a decrease in OVA signal when nonactivating beads were used, showing that this

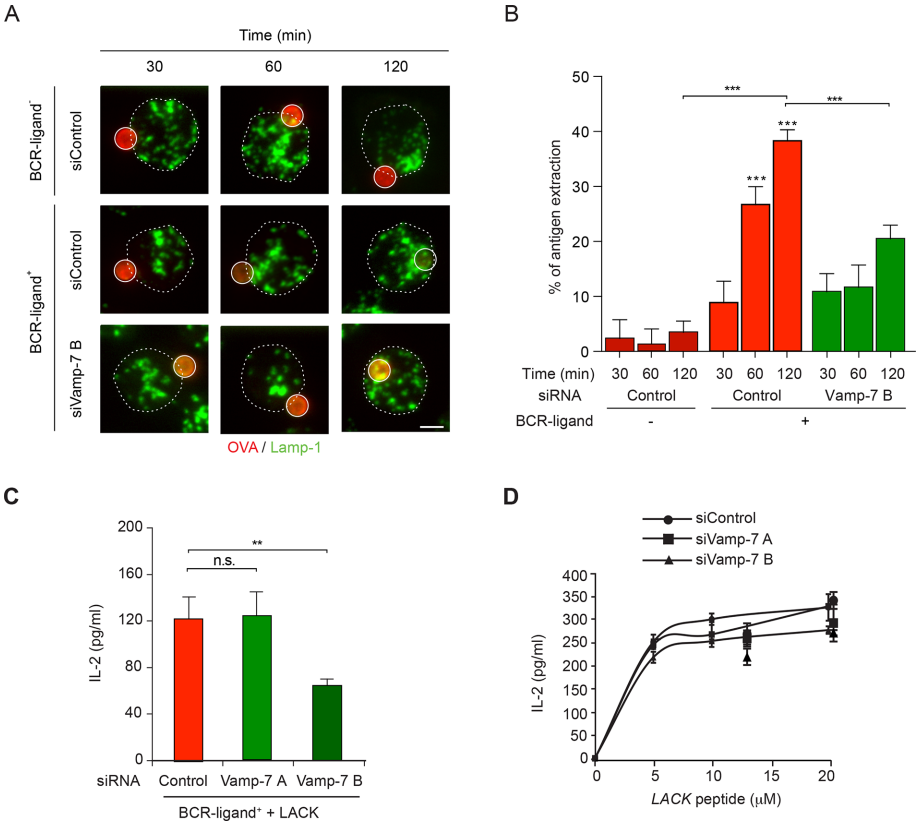

FIGURE 4: Vamp-7 is required for efficient extraction and presentation of immobilized antigens. (A) Representative 3D projections of confocal images of control and Vamp-7–silenced B-cells incubated with BCR-ligand$^+$ or BCR-ligand$^-$ beads plus OVA for different time points. Cell–bead conjugates were stained for OVA and Lamp-1. Scale bar, 3 μm. (B) Calculation of the percentage of OVA extracted from beads. Each bar represents the mean ± SEM of data pooled from two independent experiments; >45 cells per condition and per time point. siRNA BCR-ligand$^+$ vs. BCR-ligand$^-$ $p < 0.0001$; siRNA Ctrl BCR-ligand$^+$ vs. siRNA Vamp-7 B $p < 0.0001$. Unpaired *t* test. (C) Antigen presentation assay and (D) peptide control assay using control and Vamp-7–silenced cells. Mean levels of IL-2 ± SD are shown of representative experiments performed in triplicate. Two independent experiments $^{**}p = 0.0015$, *t* test.

process relies on the specific engagement of the BCR. Collectively these results suggest that silencing of Vamp-7 impairs lysosome secretion at the IS and renders B-cells less efficient in extracting immobilized Ag. To further validate our findings, we analyzed whether a decrease in Vamp-7 expression had an effect on the Ag presentation capacity of B-cells. For this, we incubated B-cells with beads coupled to specific BCR ligands plus the *Lack* antigen from *Leishmania major*. The ability of the cells to present MHC-II–peptide complexes derived from bead-associated *Lack* to a specific T-cell hybridoma was then measured by monitoring interleukin-2 (IL-2) secretion. In agreement with the results described earlier, silencing of Vamp-7 significantly decreased the capacity of B-cells to present bead-associated *Lack* antigen to T-lymphocytes (Figure 4C). Of importance, Vamp-7 silencing had no effect on the presentation of the *Lack* peptide (Figure 4D), showing that Vamp-7 does not influence B-cell/T-cell interactions. We conclude that exocytosis of secretory lysosomes at the B-cell IS is controlled by the SNARE protein Vamp-7, which is required for processing and presentation of immobilized Ag to T-lymphocytes.

Given that this v-SNARE is also involved in late endosome–to–lysosome transport (Advani *et al.*, 1999; Ward *et al.*, 2000; Fader *et al.*, 2009; Luzio *et al.*, 2010), we cannot formally exclude that the defective Ag-processing phenotype of Vamp-7–silenced B-cells may partially result from a defect in endocytic trafficking in addition to impaired lysosome secretion. Nevertheless, our data showing that lysosome secretion is impaired in Vamp-7–silenced cells favor a role for this SNARE protein in lysosome exocytosis at the plasma membrane of B-cells. Of interest, this mechanism resembles the one used by NK and cytotoxic T-cells that deliver lytic granules at the synaptic cleft to promote target killing. Here cytotoxic granule recruitment is guided by the polarization of the MTOC (Angus and Griffiths, 2013), and exocytosis occurs via specific SNARE proteins (Stow *et al.*, 2006; Krzewski *et al.*, 2011; Matti *et al.*, 2013), including Vamp-7 (Marcet-Palacios *et al.*, 2008). However, regulated secretion at the IS is a complex process involving several SNAREs, as well as their chaperones (Munc, Slp, and STXBP5) and/or Rab effector proteins, among others (Luzio *et al.*, 2007). Recent studies show that recycling of T-cell receptors (TCRs) at the IS depends on the interaction of Rab8 with Vamp-3 (Finetti *et al.*, 2015) and that cytotoxic granule fusion at the IS is a two-step process involving the prior recruitment of syntaxin-11 by Vamp-8 (Marshall *et al.*, 2015). How does Vamp-7 regulate lysosome secretion in B-cells? We propose that lysosomes must acquire this v-SNARE, most likely by intracellular fusion, in order to become competent for exocytosis. This is based on observations showing that Lamp-1$^+$ lysosomes proximal to the IS of B-cells become positive for Vamp-7 and that silencing this v-SNARE results in the accumulation of lysosomes at the synaptic membrane, which are unable to undergo secretion. Of interest, lysosomes move toward the MTOC of activated B-cells (Yuseff *et al.*, 2011), where Vamp-7$^+$ vesicles are concentrated at steady state. This process could enable lysosomes to acquire proteins required for docking/secretion, similar to the mechanism proposed for lytic granules in NK cells (Mentlik *et al.*, 2010). Recently Vamp-7 was shown to regulate the release of IL-12 from late-endocytic vesicles at the IS of activated DCs (Chiaruttini *et al.*, 2016), as well as the recruitment of LAT-containing vesicles toward TCR-activation sites at the IS of activated CD8$^+$ T-cells (Larghi *et al.*, 2013). The role of Vamp-7 in the docking of key signaling molecules and/or cytokine secretion at the IS of B-cells will now be investigated.

Recruitment of Vamp-7$^+$ vesicles to the B-cell synapse relies on Cdc42, presumably due to its control of MTOC repositioning (Yuseff *et al.*, 2011); however, local actin remodeling promoted by Cdc42 could also contribute to their stable docking, as documented in neuronal growth cones (Alberts *et al.*, 2006). In platelets, Vamp-7 promotes cell spreading by regulating exocytosis (Peters *et al.*, 2012) as well as cytoskeleton remodeling through interactions with VARP and Arp2/3 (Koseoglu *et al.*, 2015). Of interest, Arp2/3 was recently shown to be depleted from the centrosome and accumulated at the IS of activated B-lymphocytes (Obino *et al.*, 2016). Thus it is tempting to speculate that Arp2/3 could be transported to the synaptic membrane of B-cells by Vamp-7$^+$ vesicles. Indeed, we

observed a slight but significant defect in the accumulation of F-actin at the synapse of Vamp-7–silenced cells (Supplemental Figure S1H). Consequently Vamp-7 could couple lysosome secretion with actin remodeling at the IS to facilitate membrane spreading, thus allowing B-cells to capture and extract immobilized antigens more efficiently. Overall our results reveal that Vamp-7–dependent exocytosis of secretory lysosomes at the IS is critical for B-cells to acquire their Ag presentation function. Focusing on molecules that control vesicle trafficking at the IS will provide a better understanding on how B-cells acquire their effector functions.

MATERIALS AND METHODS

Cells

The mouse lymphoma cell IIA1.6 is an FcγR-defective variant of the A20 B lymphoma cell line and has the phenotype of quiescent mature B-cells expressing surface IgG2a (previously described; Lankar *et al.*, 2002). The LMR7.5 *Lack* T-cell hybridoma recognizes I-A^d/$Lack_{156–173}$ complexes. Both cell lines were cultured as reported previously (Le Roux *et al.*, 2007; Vascotto *et al.*, 2007).

Antibodies and drugs

The following antibodies were used: rat anti-mouse Lamp-1 (BD Biosciences); anti–γ-tubulin (kindly provided by Michel Bornens, UMR144, Institut Curie, Paris, France); anti–Vamp-7 (SYBL1 antibody; Novus Biologicals); and rabbit anti-GFP (Ozyme). CypHer5E was purchased from Amersham (Bioscience, Little Chalfont, United Kingdom) and used according to manufacturer's instructions.

DNA constructs and cell transfection

The plasmids encoding Vamp-7–GFP and Vamp-7–mRFP were kindly provided by Thierry Galli (Institut Jacques Monod, Paris, France). shControl and shCdc42 plasmids were previously described (Yuseff *et al.*, 2011). Nucleofactor R T16 (Lonza, Gaithersburg, MD) was used to electroporate 2.5×10^6 IIA1.6 B lymphoma cells the presence of 4 µg of plasmid DNA. After transfection of Vamp-7–GFP or –mRFP constructs, cells were cultured for 16 h before functional analysis. In the case of transfection with shCd42 or shControl plasmids, cells were incubated 72 h at 37°C before analysis and detected by the expression of GFP. For transfection with siRNA, 2×10^6 IIA1.6 cells were transfected twice (the second transfection was performed 48 h after the first) with a final concentration of 20 nM of siRNA against Vamp-7 (Mm_Sybl1_2 = siVamp-7 A), Mm_Sybl1_3 = siVamp-7 B), or luciferase (control), purchased from Qiagen.

Activation of B-cells

For B-cell–bead conjugate formation, 4×10^7 latex NH_2 beads (Polyscience) were activated with 8% glutaraldehyde (Merck) for 2 h at room temperature. Beads were then washed twice with phosphate-buffered saline (PBS) and incubated overnight with different ligands (100 µg/ml $F(ab')_2$ goat anti-mouse-IgM or $F(ab')_2$ goat anti-mouse IgG; MP Biomedicals).

Real-time quantitative reverse transcription-PCR

Total RNA was extracted using a NucleoSpin RNAII Kit (Machery Nagel). cDNA synthesis was performed using a BlueScript VILO cDNA Synthesis Kit (Invitrogen). Transcripts were quantified by real-time quantitative PCR on a Light Cycler 480 II sequence detector (Roche) with Applied Biosystems predesigned TaqMan Gene Expression Assays and qPCR Mastermix Plus (Eurogentec). We used the probes (Applied Biosystems assay identification numbers in parenthesis) Vamp-7 (Mn00807071_m1) and glyceraldehyde-3-phosphate dehydrogenase (GAPDH; Mm03302249_g1). For each sample, mRNA levels were normalized to the amount of GAPDH expression.

Immunofluorescence

B-cells activated with Ag-coated beads at a 1:1 ratio were plated on poly-L-lysine–coated glass coverslips, incubated for different times at 37°C, and fixed in 4% paraformaldehyde (PFA) for 10 min at room temperature, and PFA was quenched in PBS plus 100 mM glycine for 10 min. Fixed cells were incubated with antibodies in PBS plus 0.2% bovine serum albumin (BSA) and 0.05% saponin. Immunofluorescence images were acquired on a confocal microscope (LSM Axiovert 720; Carl ZeissMicroImaging) with a 63×/1.4 numerical aperture (NA) oil immersion objective (Carl ZeissMicroImaging).

Time-lapse analysis

For time-lapse movies, a Nikon Eclipse TE2000-U microscope equipped with a 100×/1.45 NA oil immersion objective, a PIFOC Objective stepper, a Yokogawa CSU22 confocal unit, and a Roper HQ2 charge-coupled device (CCD) camera were used. B-cells expressing the plasmids of interest attached on poly-L-lysine–coated slides were incubated in a 35-mm Iwaki-type chamber (Fluorodish) at 37°C for 20 min. Next, cell–bead conjugates were imaged and acquired using MetaMorph software every 30 s or 1 min for ~1 h.

Antigen extraction assay

Ovalbumin and $F(ab')_2$ goat anti-mouse IgM or anti-mouse IgG fragments were coupled to NH_2 beads in equal concentrations (100 µg/ml each). Cells incubated in a 1:2 ratio with Ag-coated beads were plated on poly-L-lysine coverslips at 37°C, fixed, and stained for OVA with a polyclonal antibody. The amount of OVA present on the beads was calculated by establishing a fixed area around beads in contact with cells and measuring fluorescence on three-dimensional (3D) projections obtained from the sum of each plane (ImageJ). The percentage of antigen extracted was estimated by the percentage of fluorescence intensity lost by the beads after different time points and normalized with respect to beads that were not engaged in an immune synapse for each time point.

Antigen presentation assays

The *Lack* model antigen was coupled to glutaraldehyde-activated amino beads together with $F(ab')_2$ anti–mouse IgM or anti–mouse IgG fragments in equal concentrations (see activation of B-cells). We incubated 1×10^5 IIA1.6 cells (I-A^d haplotype) with *Lack*-coated beads for 5 h at 37°C to allow uptake and processing of *Lack* antigen. The B-cells were washed, fixed with PBS plus 0.01% glutaraldehyde, quenched with PBS containing 100 mM glycine, and then incubated with 1×10^5 *Lack* T-cell hybridoma for another 24 h. Supernatants from each condition were obtained, and levels of IL-2 were measured as described (IL-2 Elisa Kit from BD Biosciences).

Measurement of cell surface levels of BCR by flow cytometry

We washed 0.5×10^6 control and Vamp-7–silenced IIA1.6 cells with ice-cold PBS plus 3% BSA and incubated them on ice for 20 min with PBS plus 3% BSA supplemented with an Alexa Fluor 488–conjugated anti–mouse IgG (Molecular Probes). Cell surface BCR levels were assessed by flow cytometry (AccuriC6; BD Biosciences).

Evanescent wave fluorescence microscopy (TIRFM)

TIRFM was performed on a Nikon Eclipse Ti inverted microscope equipped with a 100×/1.49 NA oil immersion objective and a Quantem512SC Roper electron-multiplying CCD camera at 37°C/4.5%

CO_2. B-cells expressing the plasmids of interest were attached on Ag-coated 35-mm dishes (Fluorodish) at 37°C, and images were acquired with MetaMorph software. Next, images were analyzed using ImageJ software. TrackMate v2.8.1 plug-in from Fiji (Schindelin *et al.*, 2012) was used to follow trajectories from Vamp-7$^+$ vesicles or cathepsinD-mRFP$^+$ lysosomes.

Spinning-disk microscopy

An inverted spinning-disk confocal microscope (Eclipse Ti; Roper/Nikon) with a 60×/1.4 NA oil immersion objective was used to acquire confocal images of B-cells for CypHer5E (synapse acidification) and Vamp-7/Rab6/Lamp-1–labeling experiments. MetaMorph software was used to acquire images.

Image analysis

Polarity analysis. This was performed according to (Yuseff *et al.*, 2011). Briefly, images were projected into one *z*-stack by SD method in the bright-field channel, selecting the whole cell to obtain its geometrical center of mass. The maximal fluorescence was used to position the MTOC. The weighted center of mass of different channels was used to define the average position (*x*, *y*) of the cellular components (Vamp-7$^+$ vesicles, lysosomes). Cross-correlation with a previously acquired image of the bead was used to position the bead in two dimensions. After we extracted the positions of the bead (*B*), the cell center of mass (*C*), and the MTOC (*M*) or another fluorescent marker (*F*), we computed the polarity index as projection of the vector *CM* along the vector *CB* normalized by the distance of the bead to the center of mass: the index ranges between −1 (antipolarized) and 1 (fully polarized, object on the bead). Analogously, the index for another fluorescence channel was computed as before, replacing the position (*M*) of the MTOC with that (*F*) of the center of mass of the signal in the specific channel.

Colocalization analysis. Values of Vamp-7/Rab6 and Vamp-7/Lamp-1 Pearson's *r* were determined using the JACoP plug-in of ImageJ v1.5, using Costes' automatic threshold.

Analysis of Vamp-7$^+$ TIRFM movies. Cells were transfected with plasmids encoding Vamp-7-RFP 16 h before imaging. Frames were acquired with an exposure time of 100 ms for 1 min. Vamp-7-RFP vesicle tracking was performed by using log detection to define vesicles with a diameter of 0.5 µm, as well as a first filter based on spot quality by autoselection, and also on track quality by autoselection.

Analysis of Lamp-1$^+$ vesicles. Control or Vamp-7–silenced cells were transfected with cathepsinD-mRFP (Yuseff *et al.*, 2011) 16 h before plating onto Fluorodish plates coated with F(ab')$_2$ goat anti–mouse IgG plus 0.5 µg/ml anti-CD45R/B220 for 30 min to improve cell adherence to the antigen-coated slide, as previously described (Reversat *et al.*, 2015). Images were acquired every 1 s for 3 min. The analysis was performed as follows: a sum projection was obtained using phase contrast images to establish the region of interest (ROI) corresponding to the cell contour. To determine the synapse and periphery zones, a time projection was obtained, and a circular or elliptic ROI, corresponding to the zone of lysosome accumulation in this image, was used to define the "synapse," and the remaining space between this zone and the cell contour was defined as the "periphery." Then background subtraction (radius 5) was performed. Log detection was used to identify the lysosomes, followed by a maximal fluorescence intensity filter on spots; values were adjusted according to the transfection level of each cell.

ACKNOWLEDGMENTS

M.-I.Y. is supported by a research grant from FONDECYT #1141182. D.O. was supported by fellowships from the Ecole Doctorale Bio-SPC, the Universités Paris Diderot/Paris Descartes, and the Fondation pour la Recherche Médicale (FDT20150532056). J-J.S. and J.I. were supported by fellowships from the Comision Nacional de Ciencia y Tecnologia.

REFERENCES

Advani RJ, Yang B, Prekeris R, Lee KC, Klumperman J, Scheller RH (1999). VAMP-7 mediates vesicular transport from endosomes to lysosomes. J Cell Biol 146, 765–776.

Alberts P, Rudge R, Irinopoulou T, Danglot L, Gauthier-Rouviere C, Galli T (2006). Cdc42 and actin control polarized expression of TI-VAMP vesicles to neuronal growth cones and their fusion with the plasma membrane. Mol Biol Cell 17, 1194–1203.

Angus KL, Griffiths GM (2013). Cell polarisation and the immunological synapse. Curr Opin Cell Biol 25, 85–91.

Arana E, Vehlow A, Harwood NE, Vigorito E, Henderson R, Turner M, Tybulewicz VL, Batista FD (2008). Activation of the small GTPase Rac2 via the B cell receptor regulates B cell adhesion and immunological-synapse formation. Immunity 28, 88–99.

Batista FD, Iber D, Neuberger MS (2001). B cells acquire antigen from target cells after synapse formation. Nature 411, 489–494.

Braun V, Fraisier V, Raposo G, Hurbain I, Sibarita JB, Chavrier P, Galli T, Niedergang F (2004). TI-VAMP/VAMP7 is required for optimal phagocytosis of opsonised particles in macrophages. EMBO J 23, 4166–4176.

Carrasco YR, Batista FD (2007). B cells acquire particulate antigen in a macrophage-rich area at the boundary between the follicle and the subcapsular sinus of the lymph node. Immunity 27, 160–171.

Chaineau M, Danglot L, Galli T (2009). Multiple roles of the vesicular-SNARE TI-VAMP in post-Golgi and endosomal trafficking. FEBS Lett 583, 3817–3826.

Chiaruttini G, Piperno GM, Jouve M, De Nardi F, Larghi P, Peden AA, Baj G, Muller S, Valitutti S, Galli T, Benvenuti F (2016). The SNARE VAMP7 regulates exocytic trafficking of interleukin-12 in dendritic cells. Cell Rep 14, 2624–2636.

Fader CM, Sanchez DG, Mestre MB, Colombo MI (2009). TI-VAMP/VAMP7 and VAMP3/cellubrevin: two v-SNARE proteins involved in specific steps of the autophagy/multivesicular body pathways. Biochim Biophys Acta 1793, 1901–1916.

Finetti F, Patrussi L, Galgano D, Cassioli C, Perinetti G, Pazour GJ, Baldari CT (2015). The small GTPase Rab8 interacts with VAMP-3 to regulate the delivery of recycling T-cell receptors to the immune synapse. J Cell Sci 128, 2541–2552.

Fleire SJ, Goldman JP, Carrasco YR, Weber M, Bray D, Batista FD (2006). B cell ligand discrimination through a spreading and contraction response. Science 312, 738–741.

Jahn R, Scheller RH (2006). SNAREs–engines for membrane fusion. Nat Rev Mol Cell Biol 7, 631–643.

Junt T, Moseman EA, Iannacone M, Massberg S, Lang PA, Boes M, Fink K, Henrickson SE, Shayakhmetov DM, Di Paolo NC, *et al.* (2007). Subcapsular sinus macrophages in lymph nodes clear lymph-borne viruses and present them to antiviral B cells. Nature 450, 110–114.

Koseoglu S, Peters CG, Fitch-Tewfik JL, Aisiku O, Danglot L, Galli T, Flaumenhaft R (2015). VAMP-7 links granule exocytosis to actin reorganization during platelet activation. Blood 126, 651–660.

Krzewski K, Gil-Krzewska A, Watts J, Stern JN, Strominger JL (2011). VAMP4- and VAMP7-expressing vesicles are both required for cytotoxic granule exocytosis in NK cells. Eur J Immunol 41, 3323–3329.

Lankar D, Vincent-Schneider H, Briken V, Yokozeki T, Raposo G, Bonnerot C (2002). Dynamics of major histocompatibility complex class II compartments during B cell receptor-mediated cell activation. J Exp Med 195, 461–472.

Larghi P, Williamson DJ, Carpier JM, Dogniaux S, Chemin K, Bohineust A, Danglot L, Gaus K, Galli T, Hivroz C (2013). VAMP7 controls T cell activation by regulating the recruitment and phosphorylation of vesicular Lat at TCR-activation sites. Nat Immunol 14, 723–731.

Le Roux D, Lankar D, Yuseff MI, Vascotto F, Yokozeki T, Faure-Andre G, Mougneau E, Glaichenhaus N, Manoury B, Bonnerot C, Lennon-Dumenil AM (2007). Syk-dependent actin dynamics regulate endocytic trafficking and processing of antigens internalized through the B-cell receptor. Mol Biol Cell 18, 3451–3462.

Luzio JP, Gray SR, Bright NA (2010). Endosome-lysosome fusion. Biochem Soc Trans 38, 1413–1416.
Luzio JP, Pryor PR, Bright NA (2007). Lysosomes: fusion and function. Nat Rev Mol Cell Biol 8, 622–632.
Marcet-Palacios M, Odemuyiwa SO, Coughlin JJ, Garofoli D, Ewen C, Davidson CE, Ghaffari M, Kane KP, Lacy P, Logan MR, *et al*. (2008). Vesicle-associated membrane protein 7 (VAMP-7) is essential for target cell killing in a natural killer cell line. Biochem Biophys Res Commun 366, 617–623.
Marshall MR, Pattu V, Halimani M, Maier-Peuschel M, Muller ML, Becherer U, Hong W, Hoth M, Tschernig T, Bryceson YT, Rettig J (2015). VAMP8-dependent fusion of recycling endosomes with the plasma membrane facilitates T lymphocyte cytotoxicity. J Cell Biol 210, 135–151.
Martinez-Arca S, Alberts P, Zahraoui A, Louvard D, Galli T (2000). Role of tetanus neurotoxin insensitive vesicle-associated membrane protein (TI-VAMP) in vesicular transport mediating neuriteoutgrowth. J Cell Biol 149, 889–900.
Matti U, Pattu V, Halimani M, Schirra C, Krause E, Liu Y, Weins L, Chang HF, Guzman R, Olausson J, *et al*. (2013). Synaptobrevin2 is the v-SNARE required for cytotoxic T-lymphocyte lytic granule fusion. Nat Commun 4, 1439.
Mentlik AN, Sanborn KB, Holzbaur EL, Orange JS (2010). Rapid lytic granule convergence to the MTOC in natural killer cells is dependent on dynein but not cytolytic commitment. Mol Biol Cell 21, 2241–2256.
Mitchison NA (2004). T-cell-B-cell cooperation. Nat Rev Immunol 4, 308–312.
Natkanski E, Lee WY, Mistry B, Casal A, Molloy JE, Tolar P (2013). B cells use mechanical energy to discriminate antigen affinities. Science 340, 1587–1590.
Novick P, Medkova M, Dong G, Hutagalung A, Reinisch K, Grosshans B (2006). Interactions between Rabs, tethers, SNAREs and their regulators in exocytosis. Biochem Soc Trans 34, 683–686.
Obino D, Farina F, Malbec O, Saez PJ, Maurin M, Gaillard J, Dingli F, Loew D, Gautreau A, Yuseff MI, *et al*. (2016). Actin nucleation at the centrosome controls lymphocyte polarity. Nat Commun 7, 10969.
Peters CG, Michelson AD, Flaumenhaft R (2012). Granule exocytosis is required for platelet spreading: differential sorting of alpha-granules expressing VAMP-7. Blood 120, 199–206.
Reversat A, Yuseff MI, Lankar D, Malbec O, Obino D, Maurin M, Penmatcha NV, Amoroso A, Sengmanivong L, Gundersen GG, *et al*. (2015). Polarity protein Par3 controls B-cell receptor dynamics and antigen extraction at the immune synapse. Mol Biol Cell 26, 1273–1285.
Schindelin J, Arganda-Carreras I, Frise E, Kaynig V, Longair M, Pietzsch T, Preibisch S, Rueden C, Saalfeld S, Schmid B, *et al*. (2012). Fiji: an open-source platform for biological-image analysis. Nat Methods 9, 676–682.
Schnyder T, Castello A, Feest C, Harwood NE, Oellerich T, Urlaub H, Engelke M, Wienands J, Bruckbauer A, Batista FD (2011). B cell receptor-mediated antigen gathering requires ubiquitinligaseCbl and adaptors Grb2 and Dok-3 to recruit dynein to the signaling microcluster. Immunity 34, 905–918.
Stow JL, Manderson AP, Murray RZ (2006). SNAREing immunity: the role of SNAREs in the immune system. Nat Rev Immunol 6, 919–929.
Sudhof TC, Rothman JE (2009). Membrane fusion: grappling with SNARE and SM proteins. Science 323, 474–477.
Tolar P, Sohn HW, Pierce SK (2008). Viewing the antigen-induced initiation of B-cell activation in living cells. Immunol Rev 221, 64–76.
Vascotto F, Lankar D, Faure-Andre G, Vargas P, Diaz J, Le Roux D, Yuseff MI, Sibarita JB, Boes M, Raposo G, *et al*. (2007). The actin-based motor protein myosin II regulates MHC class II trafficking and BCR-driven antigen presentation. J Cell Biol 176, 1007–1019.
Ward DM, Pevsner J, Scullion MA, Vaughn M, Kaplan J (2000). Syntaxin 7 and VAMP-7 are soluble N-ethylmaleimide-sensitive factor attachment protein receptors required for late endosome-lysosome and homotypic-lysosome fusion in alveolar macrophages. Mol Biol Cell 11, 2327–2333.
Westerberg L, Greicius G, Snapper SB, Aspenstrom P, Severinson E (2001). Cdc42, Rac1, and the Wiskott-Aldrich syndrome protein are involved in the cytoskeletal regulation of B lymphocytes. Blood 98, 1086–1094.
Yuseff MI, Lennon-Dumenil AM (2013). Studying MHC class II presentation of immobilized antigen by B lymphocytes. Methods Mol Biol 960, 529–543.
Yuseff MI, Lennon-Dumenil AM (2015). B cells use conserved polarity cues to regulate their antigen processing and presentation functions. Front Immunol 6, 251.
Yuseff MI, Pierobon P, Reversat A, Lennon-Dumenil AM (2013). How B cells capture, process and present antigens: a crucial role for cell polarity. Nat Rev Immunol 13, 475–486.
Yuseff MI, Reversat A, Lankar D, Diaz J, Fanget I, Pierobon P, Randrian V, Larochette N, Vascotto F, Desdouets C, *et al*. (2011). Polarized secretion of lysosomes at the B cell synapse couples antigen extraction to processing and presentation. Immunity 35, 361–374.